UC Davis
UC Davis Previously Published Works

Title

Telodendrimer-based nanocarriers for the treatment of ovarian cancer

Permalink

https://escholarship.org/uc/item/6nd663rz

Journal

Therapeutic Delivery, 4(10)

ISSN

2041-5990

Authors

Xiao, Kai
Suby, Nell
Li, Yuanpei
et al.

Publication Date

2013-10-01

DOI

10.4155/tde.13.91

Peer reviewed

Telodendrimer-based nanocarriers for the treatment of ovarian cancer

Kai Xiao[1], **Nell Suby**[2], **Yuanpei Li**[1], and **Kit S Lam**[*,1,3]

[1]Department of Biochemistry & Molecular Medicine, UC Davis Cancer Center, University of California Davis, Sacramento, CA 95817, USA

[2]Division of Gynecologic Oncology, Department of Obstetrics & Gynecology, UCD Cancer Center, University of California Davis, Sacramento, CA 95817, USA

[3]Division of Hematology & Oncology, Department of Internal Medicine, University of California Davis, Sacramento, CA 95817, USA

Abstract

PEG-dendritic block copolymer (telodendrimer) is a unique class of polymers with well-defined structures and tunable aggregation properties, which have been recently developed as novel micelle-based nanocarriers. This new class of nanocarrier is highly versatile, robust, multifunctional and has many unique properties for drug delivery that are superior to most other nanocarriers reported in the literature. Reversible crosslinking of micelles is able to minimize the premature drug release during circulation. These crosslinks can be reversed with endogenous and/ or exogenous stimuli. To further facilitate the precise delivery of nanoparticle drugs to cancer cells, the nanoparticles surface can be decorated with ovarian cancer targeting ligands. This review is focused on the various strategies used for the design, preparation, pharmacokinetic, biodistribution and preclinical therapeutic applications of telodendrimer-based nanocarriers for drug delivery in the treatment of ovarian cancer. Lastly, future perspectives for the development of ovarian cancer-targeting telodendrimer nanotherapeutics are also explored.

The lifetime risk for **ovarian cancer** is 1 in 70 and the prevalence is 1 in 2500 for postmeno-pausal women >50 years of age [1]. In 2013, in the US, it is estimated that 22,240 new cases were diagnosed and 14,030 women died of ovarian cancer [101]. With the increasing use of cytoreductive surgery and combination chemotherapy, 5-year survival has improved from 37% in 1974–1976 to 46% during 1999–2005 (p < 0.05) [2]. Most epithelial ovarian cancers are diagnosed at an advanced stage where the tumor has seeded the abdominal cavity (stage 3). The current therapeutic treatments for epithelial ovarian cancers include the use of combination chemotherapy with a platinum-based drug and paclitaxel (PTX). If the patient has had an optimal cytoreductive surgery (less than 1 cm of residual tumor burden) then the current gold standard of treatment involves intravenous (iv.) PTX on day 1, intraperitoneal delivery of cisplatin on day 2 and intraperitoneal PTX on day 8, repeated every 3 weeks for a total of 6 cycles [3]. Many patients are unable to complete six cycles due to the debilitating side effects of the chemotherapy. For PTX, these include hypersensitivity reactions, neurotoxicity and myelosuppression [4]. Optimizing drug

delivery while decreasing side effects is critical to improve the therapeutic nature of these drugs and also improve the quality of life of ovarian cancer patients.

Nanotechnology is an emerging field that has demonstrated great promise for the development of novel imaging and therapeutic agents for diagnosis and treatment of a variety of diseases including cancer [5]. The nanomaterials used for drug delivery include solid nanoparticles, liposomes, dendrimers, **polymeric micelles**, water soluble polymer, and protein aggregates. As the vasculature in tumors is known to be leaky to macromolecules, and the tumor lymphatic system is also deficient, nanoparticles can preferentially accumulate in the tumor site via the enhanced permeability and retention (EPR) effect [6]. Liposomal doxorubicin (Doxil®) and PTX-loaded human serum albumin nanoaggregates (Abraxane®) are among the first nanother-apeutics approved by US FDA for the treatment of cancers. In general, both of these drugs have lower toxicities than their parent drugs; however, their clinical efficacies are only marginally better than the parent drug. This could in part be explained by their relatively large size (~130 nm diameter), thus limiting tissue penetration and obviating the EPR effects. Polymeric micelles may offer some therapeutic advantages over liposomes and protein nanoaggregates as their size could be smaller (20–100 nm), and are expected to exhibit higher tumor-penetrating capacity [7].

Design of telodendrimer-based nanocarriers for ovarian cancer therapy

Criteria for effective nanocarriers for the delivery of chemotherapy drugs against ovarian cancer are: non-toxic carrier; stable inside the blood circulation with minimal premature drug release; low uptake into all normal organs and reticuloendothelial system; high tumor uptake and prolonged retention inside the tumor; ability to be taken up by tumor cells; inherent mechanisms for drug release at the tumor site or inside the tumor cells; ability to release the loaded drug on-demand; and convenient formulation protocols that can be readily carried out by clinical pharmacists at the clinic. Several novel **telodendrimer**-based nanocarrier systems have recently been developed to fulfill most of the above mentioned criteria [8,9].

Design of telodendrimers

Several novel telodendrimer-based micellar nanocarriers have recently been developed for the delivery of PTX or other hydrophobic drugs [8,10–13]. These novel nanocarriers, comprising polymers of linear PEG and oligomers of cholic acids (CA), can self-assemble under aqueous conditions to form core-shell structures that can carry PTX in the hydrophobic interior. PEG^{5k}–CA_8 is a representative telodendrimer. In the nomenclature, '5k' represents the MW of PEG (5000 Da) and '8' indicates the number of CA subunits in the telodendrimer. PEG^{5k}–CA_8 is soluble in aqueous solution and self-assembles into micelles with a size of approximately 20 nm, and is capable of encapsulating hydrophobic drugs. The azide group at the distal terminus of the PEG displaying on the surface of the micelle can be used for ligation of targeting ligands or antibodies via 'click chemistry'. The protected amino groups adjacent to the dendritic core are reserved for the conjugation of fluorescent dyes, radionuclide or additional drug molecules to the micelles. The modular design and the use of peptide chemistry to synthesize the amphiphilic polymers or telodendrimers allows one to link the CA, the hydrophilic spacers, the lysines and the PEG together in such a way that the chemical structure of the final polymer,and therefore their physicochemical properties, can be fine-tuned. Thus, one is able to control the size (ranging from 15 to 100 nm) of the monodisperse nanoparticles before and after drug loading; site-specific radioiodinate the telodendrimer; load hydrophobic drugs, radiolabel hydrophobic molecules, organic fluorescent dyes, quantum dots and supra-paramagnetic iron oxide nanoparticles into the micelle with extremely high loading capacity; and conveniently decorate the surface of the nanoparticles with the desirable targeting ligand(s) in a site-

specific manner. To the authors' knowledge, these nanocarriers have the highest PTX loading capacity (50% w/w drug/polymer) among the conventional poly-meric micelle systems reported in literature, such as the most impressive loading of PTX in PEG poly-D, L-lactatide (25% w/w) [14,15]. This novel nanoplatform is highly versatile, robust, multifunctional and its performance is superior to many reported nanocarriers [10,12]. Comparison between this oligo-cholic acid-based nanoplatform with other published micelle-based nanosystems are summarized in **Table 1.**

Reversibly crosslinked nanocarriers

The limitations of the conventional self-assem-bled micelles are gradually revealed despite the recent advances in the research of using these nanocarriers for drug delivery. These poly-meric micelles are generally thermodynamic, self-assembled systems exhibiting equilibriums between micelles and assembly units in aqueous solutions. Upon extreme dilution in the bloodstream after iv. injection, these poly-meric micelles are most likely to be dissociated to unimers due to their local concentration below the critical micelle concentration [16]. Furthermore the blood components, for example blood proteins and lipoproteins such as high-density lipoproteins, low-density lipoproteins, very low-density lipoproteins and chylomicrons, may interact with these micellar nanoparticles, leading to the premature micelle disintegration and drug release [17].

Recently, two novel reversible cross-linking strategies, disulfide (**Figure 1** [8] and boronate (**Figure 2** [9], have been developed to increase the stability of the drug-loaded nanocarriers. For *in vivo* systemic applications, these cross-linked nanocarriers are preferred as they resist premature drug release caused by the abundant lipoprotein particles (e.g., high-density lipoproteins, low-density lipoproteins, very low-density lipoproteins and chylomicrons) present in the circulation. Furthermore, these nanocarriers not only allow efficient drug delivery and release inside the tumor cells, but also can be triggered to release drug on demand by the administration of agents that have already been approved to be used in the clinic for other purposes. The disulfide crosslinks are cleaved inside the tumor cells under a reductive environment at the tumor site and inside the tumor cells, or on-demand with the administration of *N*-acetyl cysteine [8]. The boronate crosslinks are cleaved under an acidic environment inside the endosomes of the tumor cells or on demand with the administration of mannitol [9].

To design the disulfide crosslinked nanocarriers, four cysteines were introduced onto the polylysine backbone of the parent telodendrimer and generated a thiolated telodendrimer (PEG^{5k}–Cys$_4$–CA$_8$) **Figure 1**. The resulting micelles were then crosslinked via the disulfide bond formation through air oxidation [18]. The stability of the micelles was studied by monitoring the change in particle size after the addition of concentrate sodium dodecyl sulfate (SDS), which has been reported to be able to efficiently break down polymeric micelles [19]. The immediate disappearance of particle size signal of the parent PEG^{5k}–CA$_8$ micelles reflects the distinct dynamic association–dissociation property of non-crosslinked micelles. The constant particle size of the disulfide crosslinked micelles under similar conditions over a few days indicated that such crosslinked nanoparticles remained intact (**Figure 3A**.) However, in the presence of SDS and an intracellular reductive glutathione level (10 mM), the disulfide cross-linked micelle particle size signal remained unchanged for 30 min until it decreased suddenly (within 10 s), indicating rapid dissociation of the micelle when a critical number of disulfide bonds were reduced. The authors found that *N*-acetyl-cysteine (NAC), a reducing agent and a FDA-approved antidote for acetaminophen overdose, could also efficiently cleave the disulfide bonds of the crosslinked micelles, as evidenced by the complete disappearance of particle size of micelles after 40 min in the presence of SDS and NAC (10 mM). The release of the encapsulated PTX from the cross-

linked micelles was much slower than the non-crosslinked micelles (**Figure 3B**.) However, in the presence of 10 mM glutathione, the release rate increased to approximately the same as that of the non-crosslinked micelles, indicating that cleavage of the crosslinks did occur at the tumor site and particularly inside the tumor cells, where the glutathione level is high and therefore drug release is expected to occur rapidly. Alternatively, we could administer NAC at a high dose 24 h after nanotherapeutic administration to release the drug on demand.

An alternative cross-linking strategy is to exploit the well-known "reversible" covalent bond between *cis*-diol and boronic acid [20,21]. In this system two distinct telodendrimers (**Figure 2**.) are needed: PEG^{5k}–L_2–(boronicacid)$_4$–CA_{5k} and PEG^{5k}–L_2–(catechol)$_4$–CA_8. During drug loading, equal molar ratio of these telodendrimers were mixed with the drug (e.g., PTX), rotary evaporated, and rehydrated with water or saline. Covalent bonds formed between catechols and boronic acids of adjacent telodendrimers upon rehydration, resulting in the formation of stable crosslinked and drug-loaded nanocarriers measured at 21 ± 6 nm with 2 mg/ml PTX loading. Nitro-henylbo-ronic acid was chosen over phenylboronic acid because the pKa_a of nitro-phenylboronic acid is lower (6.9) and therefore the resulting crosslink is expected to be more stable at physiological pH of the blood. The authors investigated the interaction of the micelles with plasma proteins to simulate potentially destabilizing conditions for *in vivo* applications. Nitro-phenyl boronate ester crosslinked micelles (BCM4) still retained size uniformity and narrow distribution peaked at 30 nm when exposed to 50% (v/v) human plasma for 24 h. On the other hand, when mixed 1:1 with plasma, the non-crosslinked micelles (NCMs), composed of only one species of telodendrimer (either boronic acid or catechol form, but not both), demonstrated significantly broader size and bimodal distribution with populations at 81 and 237 nm, indicating the formation of large aggregates. The catechol–boronate bond weakens under acidic environment (e.g., pH 5). Therefore, it is expected that drug will be released inside endosomes of tumor cells. Nanoparticles not taken up by the tumor cells but present at the tumor sites can be readily triggered to release drug with exogenously administered mannitol. The cumulative PTX release properties of the standard non-crosslinked and the boronate crosslinked micelles were investigated in the presence of acidic pH of 5, 100 mM mannitol, or a combination of both triggering agents **(Figure 4).** The PTX release from BCM4 was significantly slower than that from NCMs at the initial 5 h. When 100 mM mannitol was added or the pH of the medium was adjusted to 5 at the 5 h time point, there was a burst of drug release from the BCM4. It should be noted that the PTX release can be further accelerated via the combination of 100 mM of mannitol and pH 5.0 **(Figure 4).** This two-stage drug release strategy can be applied *in vivo* so that there is minimal premature drug release during circulation followed by extensive release of the drugs triggered by the acidic tumor microenvironment, or upon micelle exposure to the acidic compartments of cancer cells or by the administration of mannitol.

Targeting telodendrimer-based nanocarriers

Nanoparticle drugs can be preferentially delivered to the tumor site via the EPR effect [22,23]. To further enhance the therapeutic efficacies, the nanoparticles need to be decorated with cancer-targeting ligands that can facilitate the delivery of the nanoparticle drugs into the tumor cells via receptormediated endocytosis. Integrins are cell-surface proteins that are composed of α and β subunits, which mediate cell–matrix and cell–cell adhesions [7]. For instance, the α3β1 integrin is overexpressed on the surface of ovarian cancer cells and therefore is an excellent target for ovarian cancer therapy [7]. The 'one-bead one-compound' (OBOC) combinatorial library method and whole cell binding assay were used to synthesize and rapidly identify cancer cell-targeting peptide ligands. With the OBOC library approach, resin beads display a unique peptide, which can be screened in the order of millions against the cancer cell of interest [7]. The positive beads are then isolated and the peptide's structure

is determined. The authors have used the OBOC combinatorial library method to discover and optimize a series of cyclic d-amino acid containing peptide ligands (OA02 [24], LXY1 and LXY3 [25,26]) against the a3b1 integrin that is over-expressed in many epithelial cancers including ovarian cancer [27]. Near-infrared fluorescence (NIRF) imaging illustrated that OA02 peptide has been demonstrated to bind strongly to several $\alpha3\beta1$ integrin overexpressing ovarian cancer cells and specifically target ovarian cancer xenografts (ES-2) in nude mice [24]. The telodendrimer-based nanocarriers have been decorated with OA02 peptide against the $\alpha3$ integrin receptor to improve tumor targeting specificity against ovarian cancer cells via Cu^I catalyzed cyloaddition ('click chemistry') [28]. The ligation of OA02 peptide dramatically enhanced the uptake efficiency of PEG^{5k}–CA_8 nanoparticles in SKOV-3 and ES-2 ovarian cancer cells via receptor-mediated endo-cytosis, but not in $\alpha3$ integrin-negative K562 leukemia cells. When loaded with PTX, OA02 peptide-targeted nanoparticles had significantly higher *in vitro* cytotoxicity against both SKOV-3 and ES-2 ovarian cancer cells as compared with non-targeted nanoparticles.

Pharmacokinetics & biodistribution

An understanding of the fate and biological effects of nanoparticles in animals is critical to their medical applications *in vivo*. Pharmacokinetic and organ/tissue distribution properties of nanoparticles are of great interest from a clinical point of view because of their potential uses in cancer imaging and therapy [29].

NIRF optical imaging

The *in vivo* biodistribution of DiD fluorescence dye and PTX co-loaded PEG^{5k}–CA_8 nanoparticles (DiD–PTX–NPs) was investigated in SKOV-3 ovarian cancer xenograft bearing mice via noninvasive NIRF optical imaging technology [12]. Equivalent amount of free DiD dye or DiD-PTX-NPs was intravenously injected into SKOV-3 tumor-bearing mice. As demonstrated in **Figure 5,** PEG^{5k}–CA_8 nanoparticles could gradually accumulate into tumor sites, and retain there for long periods of time (up to 72 h); whereas no obvious tumor accumulation was observed in mice injected with free DiD dye. *Ex vivo* imaging at 72 h further confirmed that PEG^{5k}–CA_8 nanoparticles mainly accumulated in the tumor tissue, which exhibited strong NIRF intensity, almost fivefold higher than the tumor uptake of free DiD control (p < 0.05). The preferential uptake of PEG^{5k}–CA_8 nanoparticles is likely due to the prolonged circulation and EPR effect. It was not surprising to observe that there was moderate uptake in the liver compared with other normal organs, which is probably attributed to the nonspecific clearance by macrophage cells (Kupffer cells) in the liver. In another set of experiments, the biodistribution of PEG^{5k}–CA_8 nanoparticles after intraperitoneal administration in an orthotopic ovarian cancer mouse model was further investigated. Mice were injected intraperitoneally with free DiD or DiD-labeled PEG^{5k}–CA_8 nanoparticles. In mice treated with free DiD, fluorescence rapidly diffused throughout the body post injection and declined to a level not distinguishable from background auto-fluorescence at 72 h post-injection. By contrast, mice injected with DiD-labeled PEG^{5k}–CA_8 nanoparticles resulted in strong fluorescence mainly localized in the abdominal region, with a majority still present at 72 h. The long-time retention effect of PEG^{5k}–CA_8 nanoparticles in the peritoneal cavity after intraperitoneal injection could be utilized to expose metastatic intraperitoneal tumor nodules and deposits to higher concentrations of the chemotherapeutic drug.

The pharmacokinetics and biodistribution of the autors recently developed disulfide-crosslinked micelles (DCMs) were investigated in an ovarian cancer xenograft mouse model [30]. To track the nanocarrier vehicle, NIRF dye BODIPY® 650/665 was conjugated to telodendrimers. To track the payload of micelles, another NIRF dye, DiD, was physically encapsulated into the core of the micelles as a drug. As illustrated in **Figure 6,** the BODIPY

signal of NCMs was rapidly eliminated from circulation and fell into the background level within 8 h post-injection, whereas the BODIPY signal of DCMs in the blood was significantly higher than that of NCMs in every occurence and sustained up to 24 h. A similar trend of circulation kinetics was also observed for the DiD-loaded NCMs and DCMs. The above profiles of elimination kinetics for both vehicle and payload indicated that the disulfide crosslinking approach significantly improves the stability of micelles and reduces the premature drug release in the blood circulation. DiD and PTX co-loaded DCMs were demonstrated to be able to preferentially accumulate in the tumor site in the subcutaneous SKOV-3 ovarian cancer xenograft mouse model. This is due to the prolonged *in vivo* circulation time of the micelles and the size-mediated EPR effect.

The *in vivo* tumor targeting specificity and tissue distribution of OA02 peptide-targeted nanoparticles (OA02-NPs) were also investigated in a SKOV-3 ovarian cancer xenograft mouse model via the NIRF optical imaging approach [28]. As illustrated in **Figure 7,** Cy5.5 fluorescent-labeled OA02-NPs were able to rapidly accumulate in the SKOV-3 ovarian cancer site after iv. injection, with much faster tumor uptake rate than that of non-targeted nanoparticles. *Ex vivo* images at 24 h indicated that the mean fluorescence intensity of tumors for OA02-NPs was approximately 1.7-fold higher than that for non-targeted nanoparticles. Histological ana lysis demonstrated that the majority of Cy5.5-labeled non-targeted nanoparticles were mainly distributed in the perivascular region, whereas OA02-NPs were able to extravasate from the tumor vasculature, penetrate deep into the interstitial space of the tumor, bind to $\alpha3$ integrin-overexpressing tumor cells, and eventually become internalized.

Radiolabeling of nanocarrier vehicles or drug payloads

Micro-single photon emission computed tomography (SPECT)/computed tomography (CT) imaging can provide an *in vivo* 3D view with higher resolution when combined with CT scanning. The authors performed a micro-SPECT/CT study in nude mice bearing subcutaneous SKOV-3 ovarian cancer xenograft with [^{125}I]-labeled, PTX-loaded 35 nm micelles (PTX–^{125}I–NM) [31]. The PEG^{5k}CA$_8$ telodendrimer was labeled with ^{125}I via the Bolton-Hunter reagent. The decay-corrected imaging indicated PTX–^{125}I–NM accumulated specifically and continuously at the tumor site and reached a peak at approximately 18–24 h post-injection. The tumor signal then decreased gradually, with substantial retention of nanomicelles in the tumor with respect to background tissue for up to 94 h post-injection. It is clear that the telodendrimer-based nanocarrier platform can target ovarian cancer xenografts with high specificity and with very low background (liver and lung) after iv. administration of the nanoparticles, which is consistent with previous results from optical imaging.

The pharmacokinetic and biodistribution profiles of ^{14}C-labeled paclitaxel (^{14}C–PTX)-loaded PEG^{5k}–CA$_8$ telodendrimer nanomicelles (^{14}C–PTX–NM) was also investigated in subcutaneous SKOV-3 ovarian cancer xenograft mouse model when compared with the clinical Cremophor formulation ^{14}C–PTX (^{14}C–Taxol®) [31]. ^{14}C–PTX–NM and ^{14}C–PTX (^{14}C–Taxol) were intravenously injected into SKOV-3 tumor-bearing mice at the dose level of 15 mg PTX/kg, respectively. The micellar formulation had higher maximum concentration of PTX than Taxol (55 μg/ml vs 21 μg/ml), and the micellar formulation also had longer terminal half-life than Taxol (70.3 h vs 46.6 h). This indicates that PTX micellar formulation exhibited prolonged blood circulation time. In the biodistribution study, PTX and its metabolites demonstrated gradual accumulation in tumor tissue, and reached a peak at around 30 min post-injection. After 24 h, the PTX concentration in tumors of animals treated with the telodendrimer nanomicelle formulation was significantly ($p < 0.05$) higher than that in other organs, including liver. In addition, the normalized tumor/muscle ratio of

radiocarbon content of ^{14}C–PTX-NM kept increasing and reached a plateau at approximately 8.5-fold 24–48 h post-injection, which was significantly higher than that of ^{14}C–Taxol (only 3.5-fold). These observations indicated that telodendrimer nanomicelles were able to enhance the tumor uptake of paclitaxel via the prolonged blood circulation and EPR effect.

Preclinical efficacy studies

Nanoparticles are emerging as an efficient tool to deliver drug therapies. They can carry chemotherapeutic drugs and can be targeted to specific cells via attached ligands or other molecular markers. The particles can be endocytosed or phagocytosed by cells allowing the encapsulated drug to be internalized. Nanoparticles of biodegradable polymers can provide controlled and targeted delivery of the drug with better efficacy and lower side effects.

In work by Xiao *et al.*, a well-defined telodendrimer has been developed to form micelles in which the drug PTX can be loaded [12]. This micellar formulation of PTX compared favorably to the free drug Taxol® and Abraxane® in *in vitro* cytotoxic studies. The maximum tolerated dose of the nanoparticle was found to be 2.5-times higher than PTX alone. In both subcutaneous and orthotopic intraperitoneal murine models of ovarian cancer, PTX-PEG^{5k}–CA$_8$ nanoparticles achieved superior toxicity profiles and antitumor effects compared with Taxol and Abraxane at equivalent PTX doses (**Figure 8**). This was attributed to their preferential tumor accumulation, and deep penetration into tumor tissue.

NCMs are limited by their premature release of the drug in the circulation. Li *et al.* created reversible DCMs in an attempt to mitigate the premature release of the drug [14]. In their work they found that the crosslinking provided stability in the bloodstream and allowed for a slower release of PTX from the DCMs compared with the NCMs. The DCMs were found to have longer *in vivo* blood circulation times, less hemolytic activities, and superior toxicity profiles in nude mice compared with NCMs. The DCMs also preferentially accumulated in the tumor sites of nude mice xenografts of SKOV-3 ovarian cancer. When compared with the free drug PTX and the NCMs, DCMs demonstrated greater efficacy at equivalent doses in an ovarian cancer mouse xenograft model (**Figure 9.**) Triggering the release of the drug by a reducing agent also enhanced the antitumor effect of the PTX–DCMs (**Figure 9.**)

An alternative approach for improving the outcome of ovarian therapy is to decorate the nanocarriers with peptide-based cancer cell surface targeting ligands for delivery of cytotoxic agents. By actively targeting the surface receptors of cancer cells, the authors speculate that there would be a higher retention of the nanoparticles and drug at the tumor site and enhanced uptake of the drug by receptor-mediated endocytosis. In work by Xiao *et al.*, micellar nanoparticles, were linked to a high-affinity 'OA02' peptide which is active against the a3 integrin receptor and is overexpressed on the surface of ovarian cancer cells [28]. When loaded with PTX, the OA02PTX-NPs displayed superior antitumor efficacy and lower systemic toxicity profiles when compared with equivalent doses of non-targeted PTX-NPs and PTX alone, in the SKOV-3 ovarian cancer xenograft mouse model (**FITURE 10.**) In unpublished work by this same group, at a dose of 20 mg PTX/kg, the PTX-loaded boronate cross-linked micelles (BCM–PTX) decorated with or without another ovarian cancer targeting peptide (targeting BCM–PTX) exhibited superior tumor growth inhibition and longer survival time compared with free PTX formulaton (Taxol) at its maximum tolerated dose of 10 mg/ kg in an intraperitoneal mouse model of ovarian cancer. The targeting BCM–PTX and targeting BCM–PTX with mannitol trigger demonstrated improved tumor growth inhibition and longer survival times than the BCM–PTX group.

Conclusion & future perspective

Nanoparticles for drug delivery are a promising field for delivering well-studied chemotherapeutics, but with the benefit of less systemic toxicity and with an increased maximum tolerated dose for ovarian cancer therapy. The nanocarriers reviewed here have the highest PTX loading capacity and are a versatile and multifunctional nanoplatform. The reversibly crosslinked nanocarriers provide efficient drug delivery inside the tumor cells, but also can allow for a triggered drug release by *N*-acetyl cysteine or mannitol. The benefit of a peptidebased cancer cell surface targeting agent is that the drug can be delivered intracellularly while specifically targeting the tumor rather than normal tissue. Nanocarriers composed of telodendrimers can preferentially deliver the drug to the tumor site when the telodendrimers are attached with cancer cell-targeting ligands. This provides an improved therapeutic response in preclinical mouse xenograft models. Besides peptides, small molecules such as folate [32]), nucleic acid aptamers [33] and antibodies [34] have been also used as cancer targeting ligands for the delivery of nanoparticle drugs.

A future goal is developing specific ligands that will target most of the epithelial ovarian cancers. The challenge in this is particularly troublesome in ovarian cancer. The term ovarian cancer is misleading. For many years we have thought of 'ovarian cancer' as one disease, despite varying stages of diagnosis, disease spread, disease progression and histologic types. With the possible exception of poly(ADP-ribose) polymerase inhibitors and angiogenesis inhibitors (Avastin®), single-agent, molecularly targeted therapies have only yielded small increments in progression-free survival in ovarian cancers. With the identification of new cell receptors and targeting ligands, the next step would be to test individual tumors for receptors that are overexpressed and formulate corresponding targeting ligands decorated nanoparticles for the delivery of traditional chemotherapeutics. The improved toxicity profile of reversible crosslinked nanocarriers would allow for additional cycles of chemotherapy to be administered for improved cell log kill, and the addition of targeted ligands can enhance the overall therapeutic response of nanotherapeutic drugs.

Acknowledgments

References/Website

Papers of special note have been highlighted as:

■ of interest

■■ of considerable interest

1. Jemal A, Siegel R, Xu J, Ward E. Cancer statistics, 2010. CA Cancer J. Clin. 2010; 60(5):277–300. [PubMed: 20610543]

2. Bast RC Jr. Molecular approaches to personalizing management of ovarian cancer. Ann. Oncol. 2011; 22(Suppl. 8):viii5–viii15. [PubMed: 22180401]

3. Marchetti C, Pisano C, Facchini G, et al. First-line treatment of advanced ovarian cancer: current research and perspectives. Expert Rev. Anticancer Ther. 2010; 10(1):47–60. [PubMed: 20014885]

4. Mayerhofer K, Kucera E, Zeisler H, Speiser P, Reinthaller A, Sevelda P. Taxol as second-line treatment in patients with advanced ovarian cancer after platinum-based first-line chemotherapy. Gynecol. Oncol. 1997; 64(1):109–113. [PubMed: 8995557]

5. Davis ME, Chen ZG, Shin DM. Nanoparticle therapeutics: an emerging treatment modality for cancer. Nat. Rev. Drug Discov. 2008; 7(9):771–782. [PubMed: 18758474]

6■. Matsumura Y, Maeda H. A new concept for macromolecular therapeutics in cancer chemotherapy: mechanism of tumoritropic accumulation of proteins and the antitumor agent smancs. Cancer Res. 1986; 46(12 Pt 1):6387–6392. [PubMed: 2946403] [First paper to describe the enhanced permeability and retention effect.]

7. Bae Y, Nishiyama N, Fukushima S, Koyama H, Yasuhiro M, Kataoka K. Preparation and biological characterization of polymeric micelle drug carriers with intracellular pH-triggered drug release property: tumor permeability, controlled subcellular drug distribution, and enhanced *in vivo* antitumor efficacy. Bioconjug. Chem. 2005; 16(1):122–130. [PubMed: 15656583]

8■. Xiao K, Li Y, Luo J, et al. The effect of surface charge on *in vivo* biodistribution of PEG-oligocholic acid based micellar nanoparticles. Biomaterials. 2011; 32(13):3435–3446. [PubMed: 21295849] [Systematically investigates the effect of surface charge on the biodistribution of telodendrimer-based micelles.]

9■■. Li Y, Xiao W, Xiao K, et al. Well-defined, reversible boronate crosslinked nanocarriers for targeted drug delivery in response to acidic pH values and *cis*-diols. Angew. Chem. Int. Ed. Engl. 2012; 51(12):2864–2869. [PubMed: 22253091] [Reports the reversible boronate crosslinking of telodendrimer-based micelles.]

10. Li Y, Xiao K, Luo J, Lee J, Pan S, Lam KS. A novel size-tunable nanocarrier system for targeted anticancer drug delivery. J. Control. Release. 2010; 144(3):314–323. [PubMed: 20211210]

11. Li XR, Yang ZL, Yang KW, et al. Self-assembled polymeric micellar nanoparticles as nanocarriers for poorly soluble anticancer drug Ethaselen. Nanoscale Res. Lett. 2009; 4(12):1502–1511. [PubMed: 20652138]

12■■. Xiao K, Luo J, Fowler WL, et al. A self- assembling nanoparticle for paclitaxel delivery in ovarian cancer. Biomaterials. 2009; 30(30):6006–6016. [PubMed: 19660809] [The first paper to report PEG-oligocholic acid telodendrimer for drug delivery.]

13. Luo J, Xiao K, Li Y, et al. Well-defined, size- tunable, multifunctional micelles for efficient paclitaxel delivery for cancer treatment. Bioconjug. Chem. 2010; 21(7):1216–1224. [PubMed: 20536174]

14. Li Y, Xiao K, Luo J, Lee J, Pan S, Lam KS. A novel size-tunable nanocarrier system for targeted anticancer drug delivery. J. Control. Release. 2010; 144(3):314–323. [PubMed: 20211210]

15. Gaucher G, Marchessault RH, Leroux JC. Polyester-based micelles and nanoparticles for the parenteral delivery of taxanes. J. Control. Release. 2010; 143(1):2–12. [PubMed: 19925835]

16. Rijcken CJ, Snel CJ, Schiffelers RM, van Nostrum CF, Hennink WE. Hydrolysable core-crosslinked thermosensitive polymeric micelles: synthesis, characterisation and *in vivo* studies. Biomaterials. 2007; 28(36):5581–5593. [PubMed: 17915312]

17. Li Y, Budamagunta MS, Luo J, Xiao W, Voss JC, Lam KS. Probing of the assembly structure and dynamics within nanoparticles during interaction with blood proteins. ACS Nano. 2012; 6(11):9485–9495. [PubMed: 23106540]

18. Matsumoto S, Christie RJ, Nishiyama N, et al. Environment-responsive block copolymer micelles with a disulfide cross-linked core for enhanced siRNA delivery. Biomacromolecules. 2009; 10(1):119–127. [PubMed: 19061333]

19. Koo AN, Lee HJ, Kim SE, et al. Disulfide- cross-linked PEG-poly(amino acid)s copolymer micelles for glutathione-mediated intracellular drug delivery. Chem. Commun. (Camb.). 2008; (48):6570–6572. [PubMed: 19057782]

20. Mulla HR, Agard NJ, Basu A. 3-Methoxycarbonyl-5-nitrophenyl boronic acid: high affinity diol recognition at neutral pH. Bioorg. Med. Chem. Lett. 2004; 14(1):25–27. [PubMed: 14684290]

21. Ren L, Liu Z, Dong M, Ye M, Zou H. Synthesis and characterization of a new boronate affinity monolithic capillary for specific capture of *cis*-diol-containing compounds. J. Chromatogr. A. 2009; 1216(23):4768–4774. [PubMed: 19419728]

22. Nie S, Xing Y, Kim GJ, Simons JW. Nanotechnology applications in cancer. Annu. Rev. Biomed. Eng. 2007; 9:257–288. [PubMed: 17439359]

23. Gao ZG, Lukyanov AN, Singhal A, Torchilin VP. Diacyllipid-polymer micelles as nanocarriers for poorly soluble anticancer drugs. Nano Lett. 2002; 2(9):979–982.

24. Aina OH, Marik J, Gandour-Edwards R, Lam KS. Near-infrared optical imaging of ovarian cancer xenografts with novel alpha 3-integrin binding peptide "OA02". Mol. Imaging. 2005; 4(4):439–447. [PubMed: 16285906]

25. Yao N, Xiao W, Wang X, et al. Discovery of targeting ligands for breast cancer cells using the one-bead one-compound combinatorial method. J. Med. Chem. 2009; 52(1):126–133. [PubMed: 19055415]

26. Yao N, Xiao W, Meza L, Tseng H, Chuck M, Lam KS. Structure-activity relationship studies of targeting ligands against breast cancer cells. J. Med. Chem. 2009; 52(21):6744–6751. [PubMed: 19835381]

27. Mizejewski GJ. Role of integrins in cancer: survey of expression patterns. Proc. Soc. Exp. Biol. Med. 1999; 222(2):124–138. [PubMed: 10564536]

28■■. Xiao K, Li Y, Lee JS, et al. 'OA02' peptide facilitates the precise targeting of paclitaxel-loaded micellar nanoparticles to ovarian cancer *in vivo*. Cancer Res. 2012; 72(8):2100–2110. [PubMed: 22396491] [Utilizes the peptide ligand to precisely deliver micellar nanocarrier to ovarian cancer.]

29. Moghimi SM, Hunter AC, Andresen TL. Factors controlling nanoparticle pharmacokinetics: an integrated analysis and perspective. Annu. Rev. Pharmacol. Toxicol. 2012; 52:481–503. [PubMed: 22035254]

30■■. Li Y, Xiao K, Luo J, et al. Well-defined, reversible disulfide cross-linked micelles for on-demand paclitaxel delivery. Biomaterials. 2011; 32(27):6633–6645. [PubMed: 21658763] [Reports the reversible disulfide crosslinking of telodendrimer-based micelles.]

31■. Xiao W, Luo J, Jain T, et al. Biodistribution and pharmacokinetics of a telodendrimer micellar paclitaxel nanoformulation in a mouse xenograft model of ovarian cancer. Int. J. Nanomedicine. 2012; 7:1587–1597. [PubMed: 22605931] [Microsingle-photon emission computed tomography/computed tomography imaging and radiolabeling were used to study the pharmacokinetics and biodistribution of telodendrimer-based micelles.]

32. Werner ME, Karve S, Sukumar R, et al. Folate-targeted nanoparticle delivery of chemo- and radiotherapeutics for the treatment of ovarian cancer peritoneal metastasis. Biomaterials. 2011; 32(33):8548–8554. [PubMed: 21843904]

33. Gao H, Qian J, Yang Z, et al. Whole-cell SELEX aptamer-functionalised poly(ethyleneglycol)-poly(epsilon–CAprolactone) nanoparticles for enhanced targeted glioblastoma therapy. Biomaterials. 2012; 33(26):6264–6272. [PubMed: 22683171]

34. Peng XH, Wang Y, Huang D, et al. Targeted delivery of cisplatin to lung cancer using ScFvEGFR-heparin-cisplatin nanoparticles. ACS Nano. 2011; 5(12):9480–9493. [PubMed: 22032622]

35■. Xiao K, Luo J, Li Y, Xiao W, Lee JS, Gonik AM, Lam KS. The passive targeting of polymeric micelles in various types and sizes of tumor models. Nanosci. Nanotechnol. Lett. 2010; 2(2):7. [Effects of tumor types and sizes on the enhanced permeability and retention effect of telodendrimer micelles.]

36. Musacchio T, Laquintana V, Latrofa A, Trapani G, Torchilin VP. PEG-PE micelles loaded with paclitaxel and surface-modified by a PBR-ligand: synergistic anticancer effect. Mol. Pharm. 2009; 6(2):468–479. [PubMed: 19718800]

37. Batrakova EV, Kabanov AV. Pluronic block copolymers: evolution of drug delivery concept from inert nanocarriers to biological response modifiers. J. Control. Release. 2008; 130(2):98–106. [PubMed: 18534704]

38. Liggins RT, Burt HM. Polyether-polyester diblock copolymers for the preparation of paclitaxel loaded polymeric micelle formulations. Adv. Drug Deliv. Rev. 2002; 54(2):191–202. [PubMed: 11897145]

39. Matsumura Y. Poly (amino acid) micelle nanocarriers in preclinical and clinical studies. Adv. Drug Deliv. Rev. 2008; 60(8):899–914. [PubMed: 18406004]

40. Huh KM, Min HS, Lee SC, Lee HJ, Kim S, Park K. A new hydrotropic block copolymer micelle system for aqueous solubilization of paclitaxel. J. Control. Release. 2008; 126(2):122–129. [PubMed: 18155795]

101. National Cancer Institute. Ovarian cancer. 2013. www.cancer.gov/cancertopics/types/ovarian

Executive summary

Ovarian cancer targeting crosslinked telodendrimer-based micelles

□ The telodendrimer-based micelle is a unique class of nanocarriers, which is highly versatile, robust and multifunctional. The reversible crosslink of micelles is able to minimize the premature drug release. The decoration of targeting ligands will facilitate the precise homing of nanocarries to ovarian cancer cells.

Pharmacokinetics & biodistribution of telodendrimer-based nanocarriers

□ Telodendrimer-based nanocarriers are able to preferentially deliver anticancer drugs into ovarian cancer via the prolonged blood circulation and enhanced permeability and retention effect.

Preclinical validation of telodendrimer nanoformulations

□ Telodendrimer-based micelle nanoformulations are not only more efficacious, but also less toxic than the current clinical preparations in preclinical ovarian cancer xenograft mouse models.
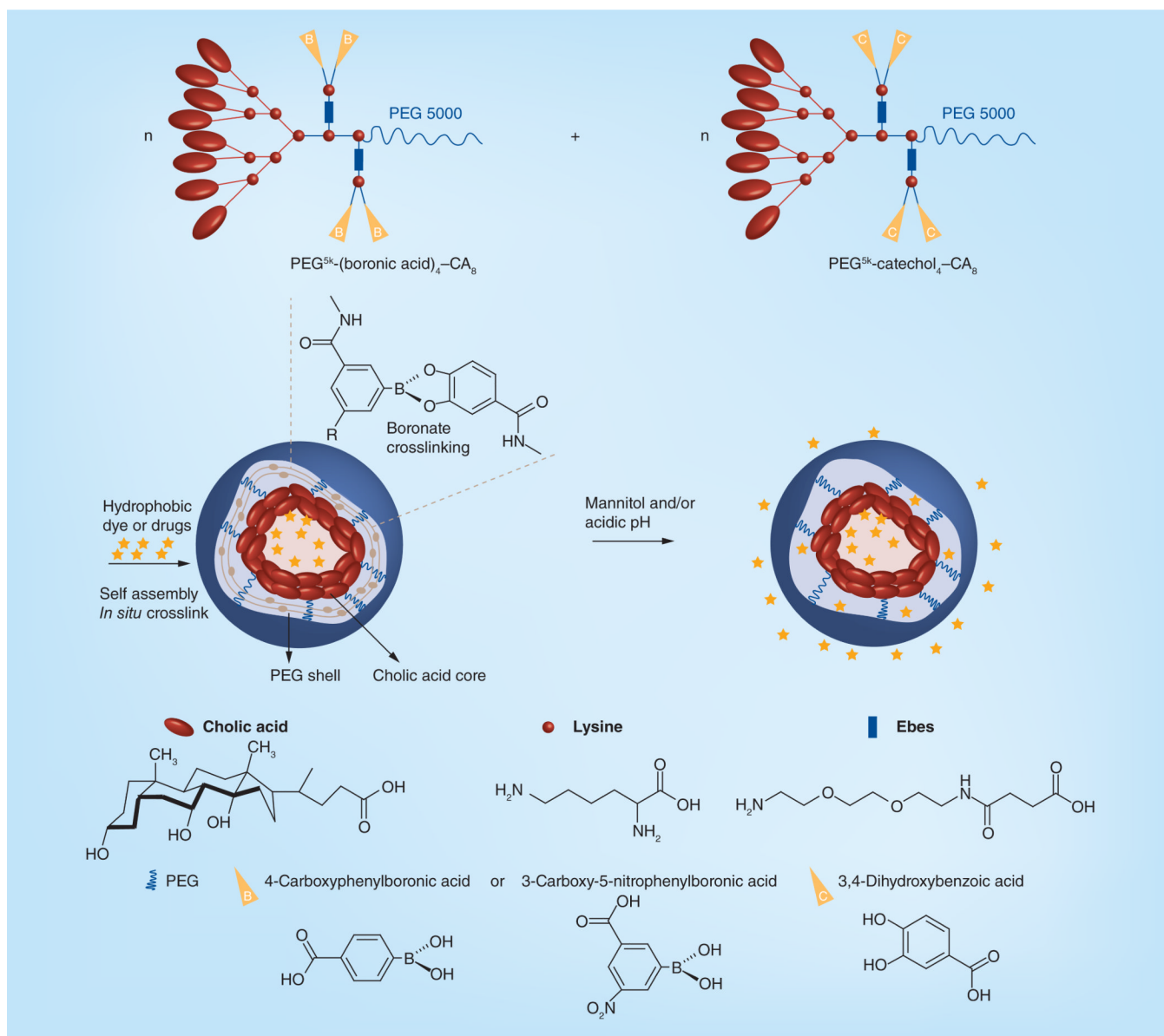
Key Terms

Ovarian cancer: Cancerous growth arising from different parts of the ovary.

**Polymeric micelles:** Micelles formed by amphiphilic copolymers.

**Telodendrimer:** PEG-dendritic block copolymer.

Figure 1.
Disulfide crosslinked micelles formed by oxidization of thiolated telodendrimer PEG^{5k}-Cys$_4$-L$_8$–CA$_8$ after self-assembly.
Reproduced with permission from [8] © Elsevier (2011).

Figure 2.
Telodendrimer pair (PEG^{5k}–[boronic acid/catechol]$_4$–cholic acid-8 [CA$_8$]) and the resulting boronate crosslinked micelles in response to mannitol and/or acidic pH.
Reproduced with permission from [9] © Wiley-VCH Verlag GmbH & Co. KGaA (2012).
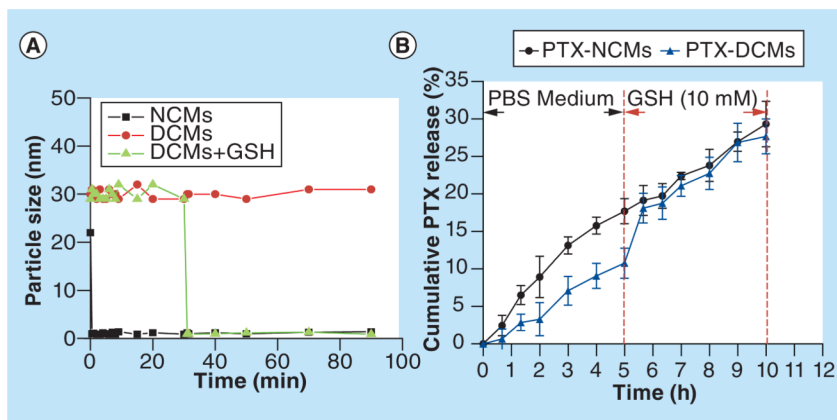
Figure 3.
The stability and GSH-responsive drug release profiles of disulfide-crosslinked micelles. (A) The stability in particle size of NCMs and DCMs in the presence of 2.5 mg/ml sodium dodecyl sulfate measured by DLS. **(B)** GSH-responsive PTX release profiles of PTX–DCMs by adding GSH (10 mM) at a specific release time (5 h) compared with PTX–NCMs [8]. DCM: Disulfide-crosslinked micelle; NCM: Non-crosslinked micelle; PTX: Paclitaxel. Reproduced with permission from [8] © Elsevier (2011).
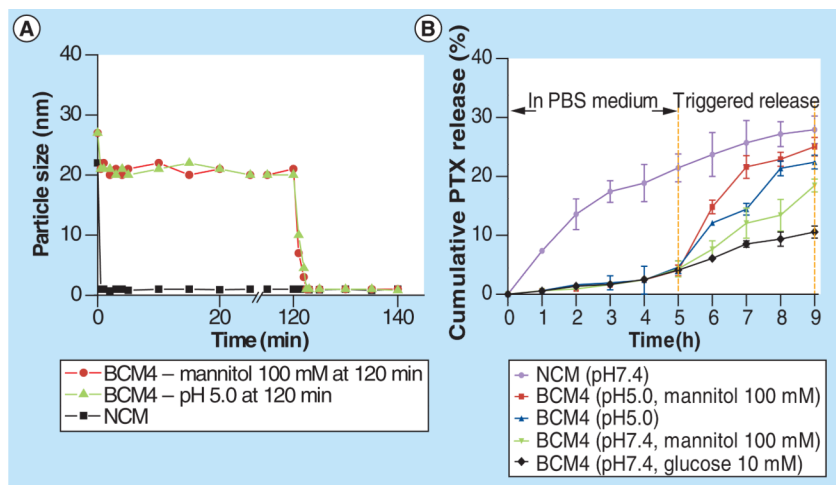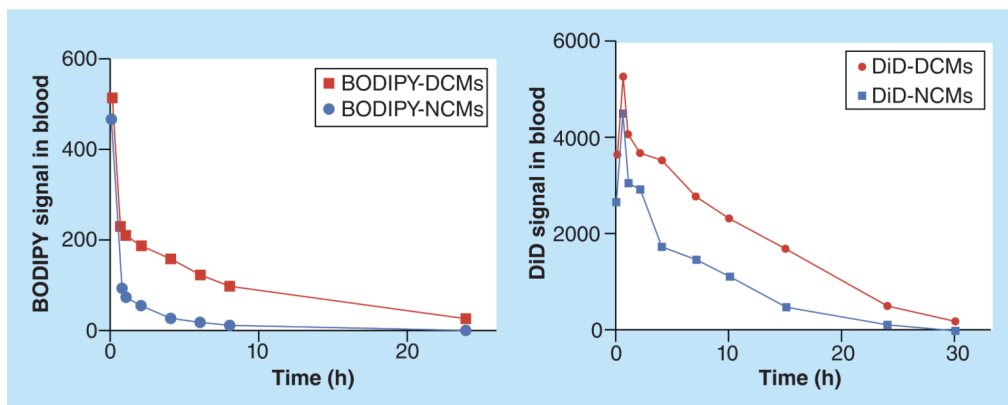
Figure 4.
The stability and drug release profiles of BCM4 with/without the presence of diols or low pH. (A) Continuous dynamic light scattering measurements of NCMs in SDS and BCM4 in SDS for 120 min, at which time mannitol was added or pH of the solution was adjusted to 5.0 (see arrow). **(B)** pH- and diol-responsive PTX release profiles of BCM4 by treating with diols (mannitiol and glucose) and/or pH 5.0 at 5 h compared with that of NCMs [9]. NCM: Non-crosslinked micelle; PTX: Paclitaxel.
Reproduced with permission from [9] © Wiley-VCH Verlag GmbH & Co. KGaA (2012).
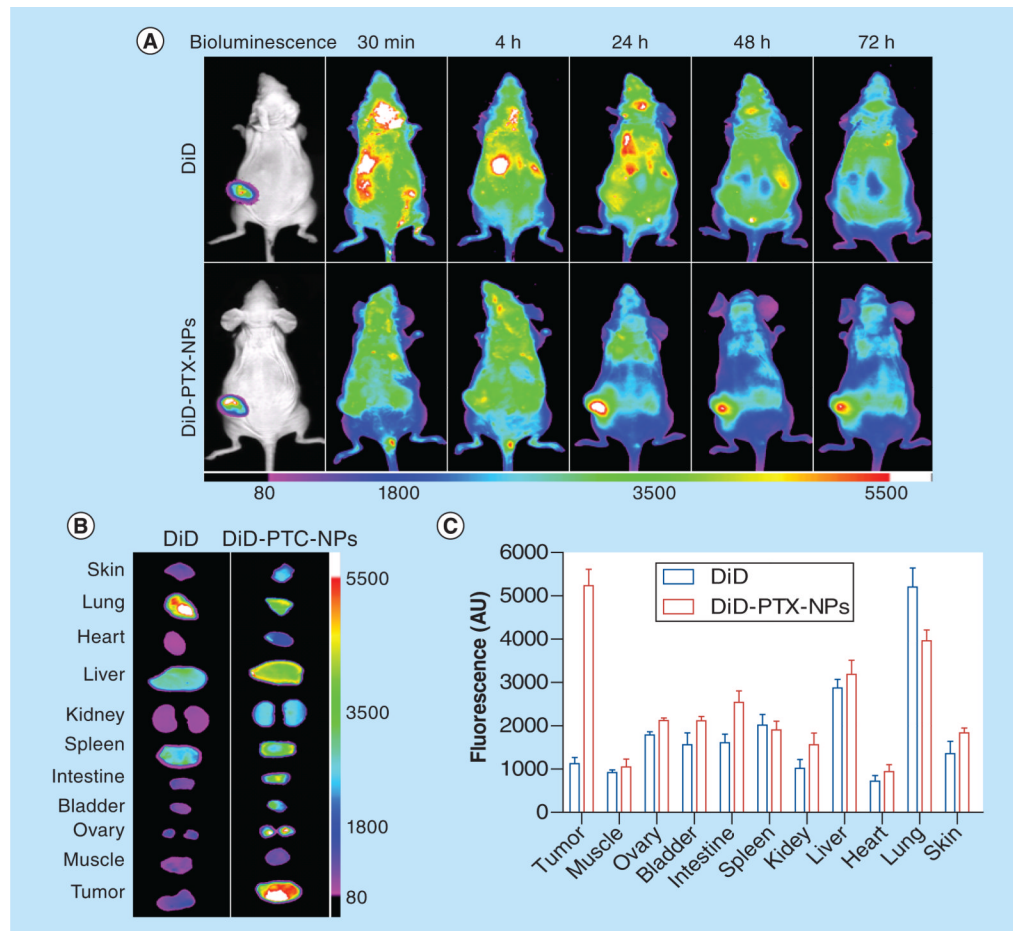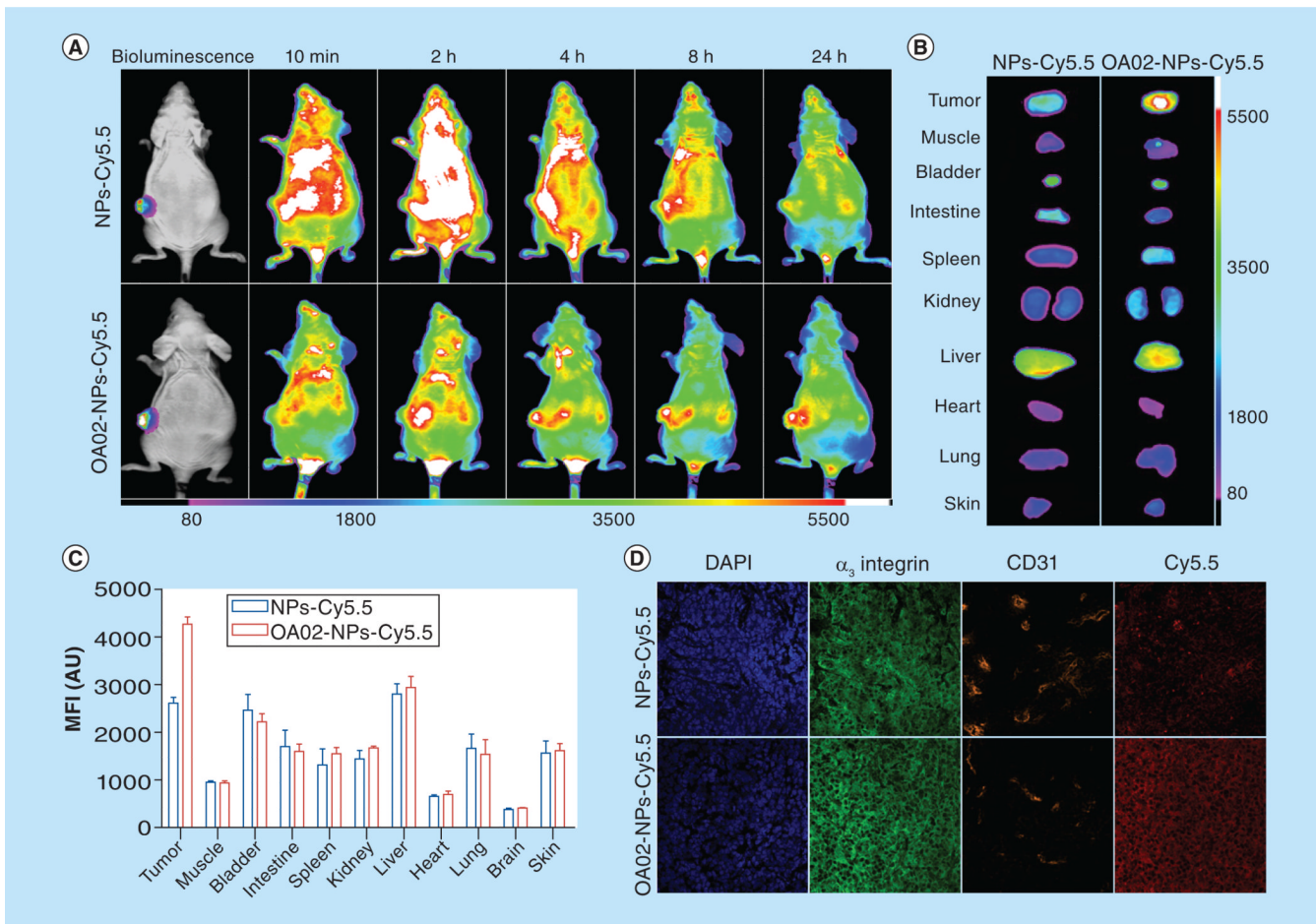
Figure 5.
In vivo and *ex vivo* near-infrared fluorescence imaging of PEG^{5k}–CA_8 nanoparticles biodistribution after intravenous injection in subcutaneous luciferase-expressing SKOV-3 tumor-bearing mice. (A) *In vivo* optical images of real-time tumor targeting characteristics of PEG^{5k}–CA_8 nanoparticles. The location and possible metastasis of the luciferase-expressing SKOV-3 tumors were determined with bioluminescence by injecting intraperitoneally 150 mg/kg luciferin. Tumor bearing mice were injected intravenously with the equivalent amount of free DiD dye or DiD–PTX–NPs. The optical imaging was obtained using Kodak multimodal imaging system IS2000MM equipped with an excitation bandpass filter at 625 nm and an emission at 700 nm. **(B)** Representative *ex vivo* optical images of tumors and organs of luciferase-expressing SKOV-3 bearing mice sacrificed at 72 h. **(C)** Quantitative fluorescence intensities of tumors and organs from *ex vivo* images (*n* = 3). NP: Nanoparticle; PTX: Paclitaxel.
Reproduced with permission from [12] © Elsevier (2009).

Figure 6.
Fluorescence signal of (A) BODIPY-labeled and (B) DiD-loaded DCMs and NCMs in the blood collected at different time points after intravenous injection in the nude mice. DCM: Disulfide-crosslinked micelle; NCM: Non-crosslinked micelle.
Reproduced with permission from [8] © Elsevier (2011).

Figure 7.

In vivo (A) and *ex vivo* (B) NIRF optical imaging of Cy5.5-labeled nanoparticles or OA02-NPs biodistribution after intravenous injection in subcutaneous SKOV-3-luc ovarian cancer xenograft mouse model. (C) Quantitate fluorescence intensities of tumors and organs from *ex vivo* images at 24 h post-injection. **(D)** Histologic ana lysis of NPs or OA02-NPs distribution (Cy5.5, red) in tumor cryosections.

NP: Nanoparticle.

Reproduced with permission from [28] © the American Association for Cancer Research, Inc. (2012).
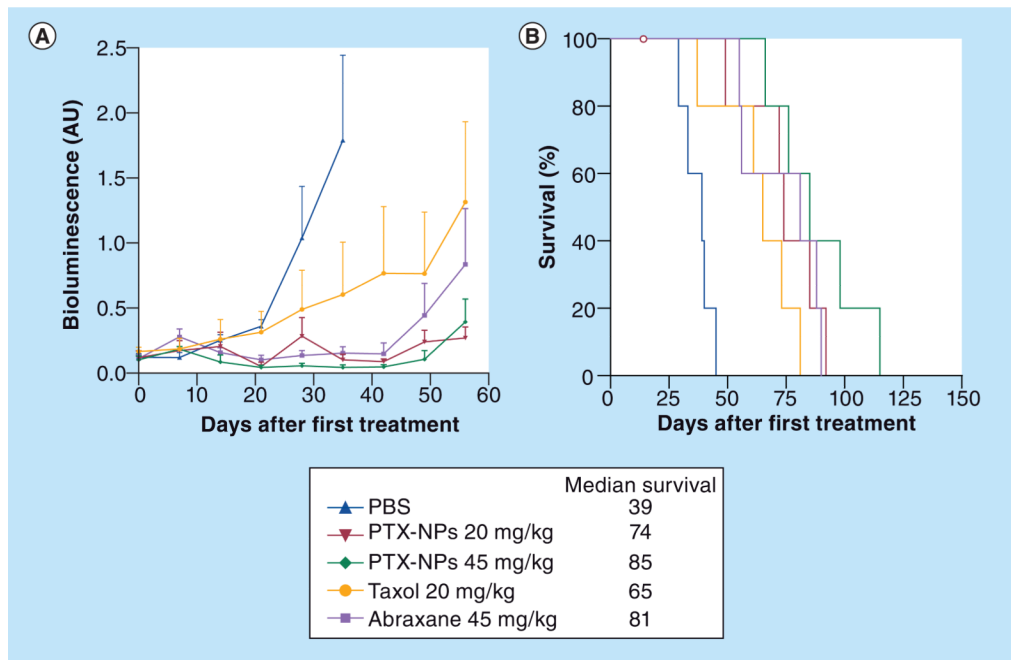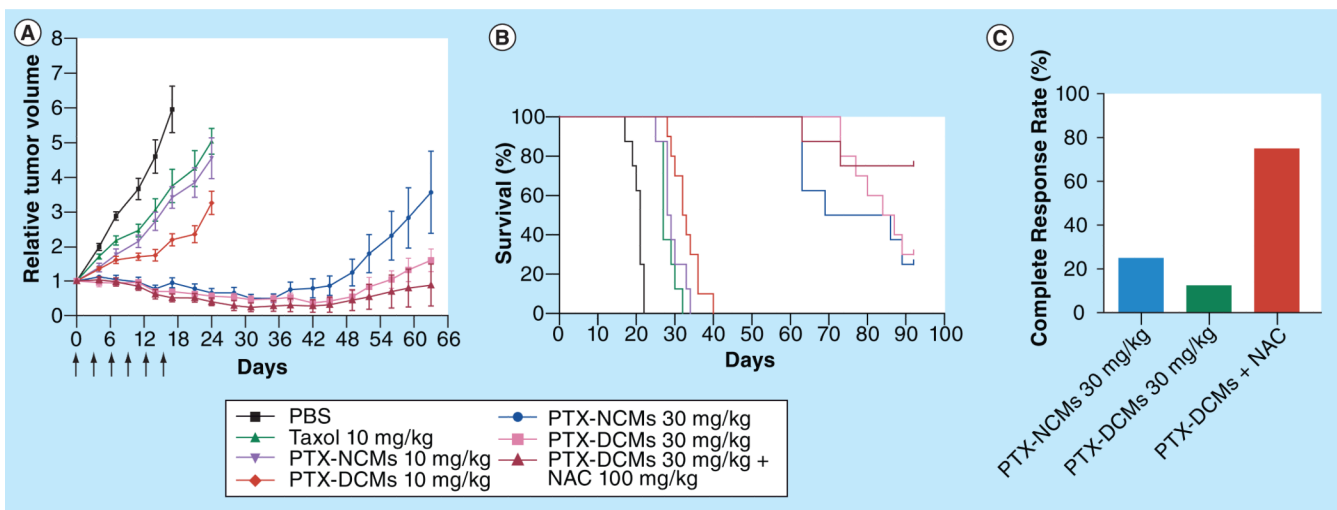
Figure 8.
The antitumor efficacy after intraperitoneal therapy of different paclitaxel formulations and noninvasive bioluminescence imaging in a murine model of peritoneal disseminated ovarian cancer. (A) Bioluminescence emitted by luciferase-expressing SKOV-3-luc cancer cells at different time points after treatment. Peritoneal SKOV-3-luc tumors bearing mice received a total of five intraperitoneal injections of Taxol®, Abraxane® and PTX–PEG^{5k}–CA$_8$ NPs on day 0, 4, 8, 12 and 16. Control groups received PBS only. Signals from the entire abdominal region of each mouse were quantified, and background was subtracted by measuring same sized ROIs in areas without light emission. **(B)** Survival of mice in different treatment groups. Open circle represents censored data point secondary to a death during anesthesia (i.e., not tumor-related).
NP: Nanoparticle; PTX: Paclitaxel.
Reproduced with permission from [12] © Elsevier (2009).

Figure 9.
Preclinical therapeutic efficacy of PTX-DCMs for ovarian cancer. (A) *In vivo* antitumor efficacy after intravenous treatment of different PTX formulations in the subcutaneous mouse model of SKOV-3 ovarian cancer. Tumor-bearing mice were administered intravenous with PBS (control) and different PTX formulations on days 0, 3, 6, 9, 12, 15 when tumor volume reached ~100–200 mm^3 (n = 8). **(B)** Survival of mice in different treatment groups. **(C)** Complete tumor response rate of mice treated with 30 mg/kg PTX–NCMs and PTX–DCMs with or without the trigger release by NAC.
DCM: Disulfide-crosslinked micelle; NAC: *N*-acetyl-cysteine; NCM: Non-crosslinked micelle; PTX: Paclitaxel.
Reproduced with permission from [8] © Elsevier (2011).
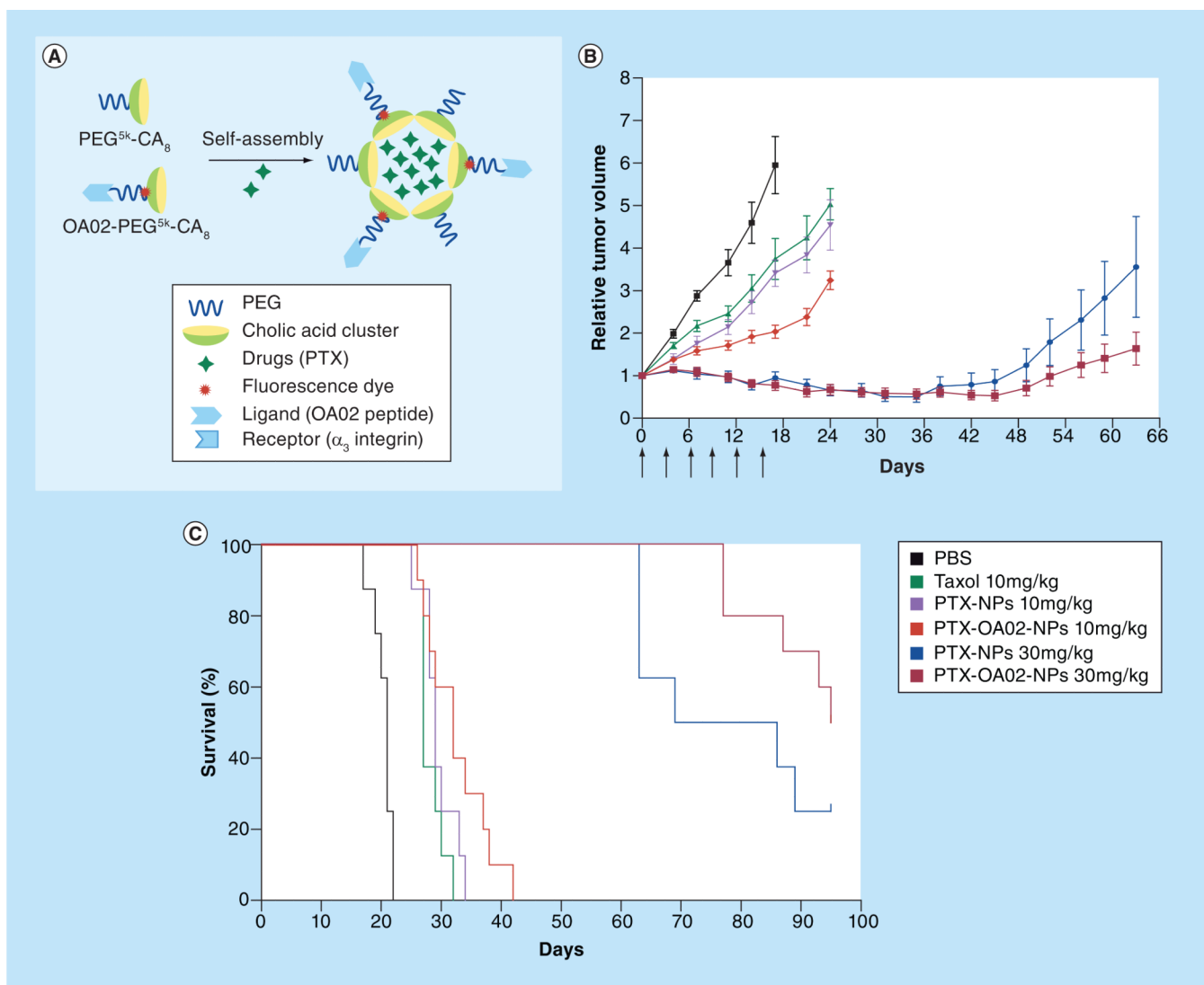
Figure 10.
Targeting ligand OA02-decorated nanoparticles for the treatment of ovarian cancer. (A) The preparation of ovarian cancer targeting NPs by the self-assembly of blank/OA02-functionalized telodendrimers. The OA02 peptides presented on the surface of targeted NPs are able to specifically recognize and bind the α-3 integrin receptors, which are overexpressed on the cell membrane of ovarian cancer cells. **(B)** *In vivo* tumor growth inhibition and **(C)** Kaplan-Meier survival curves of SKOV-3 tumor bearing mice after the intravenous treatment of various PTX formulations. Tumor-bearing mice were administered intravenously with PBS (control), Taxol® (10 mg/kg), PTX-NPs (10 and 30 mg/kg) and OA02-PTX-NPs (10 and 30 mg/kg), respectively, every 3 days on days 0, 3, 6, 9, 12 and 15 for a total of six doses. Data represent mean ± SEM (n = 8–10).
NP: Nanoparticle; PTX: Paclitaxel.
Reproduced with permission from [28] © The American Association for Cancer Research, Inc. (2012).

Table 1

Comparison of various therapeutic nanomicellar systems reported in the literature.

Nanomicellar systems	Synthetic chemistry[†]	Modular design	Polydispersity Index[‡]	Site-specific modification	Post-crosslinking[§]	Loading capacity	Stability (with drug)	Ref.
Telodendrimer	Peptide chemistry	Yes	<1.05	Yes, multiple sites	Yes	High	>6 months	[8,10,12,13,35,30]
PEG-PE	Conjugation	No	<1.05	No	No	Fair to good	Days	[36]
PEO-PPO-PEO	AP	No	~1.1	No	No	Good	Days	[37]
PEG-P(ester)	ROP	No	1.2-1.4	No	No	High	Hours to days	[38]
PEG-P(amino acid)	ROP	No	>1.2	Nonspecific	Yes	Good to high	Days to months	[39]
Hydrotropic micelle	ATRP	No	~1.1	No	No	High	Days to months	[40]

AP: Anionic polymerization: ATRP: Atom transfer radical polymerization; PE: Phosphatidylethanolamine; PEO: Polyethylene oxide; PPO: Polypropylene oxide; ROP: Ring opening polymerization.

[†] Polymerization reactions are more difficult to control than the single-step specific organic reactions, therefore polymerization always leads to the polydispersed distribution of the polymer chains.

[‡] Polydispersity Index 1.0 indicates narrow dispersed population of polymer chains.

[§] Crosslinking of telodendrimers to increase micelle stability in the telodendrimer platform.